



Nanocellulose for Energy Storage Systems: Beyond the Limits of Synthetic Materials

Jung-Hwan Kim, Donggue Lee, Yong-Hyeok Lee, Wenshuai Chen,* and Sang-Young Lee*

The ongoing surge in demand for high-performance energy storage systems inspires the relentless pursuit of advanced materials and structures.

Components of energy storage systems are generally based on inorganic/metal compounds, carbonaceous substances, and petroleum-derived hydrocarbon chemicals. These traditional materials, however, may have difficulties fulfilling the ever-increasing requirements of energy storage systems. Recently, nanocellulose has garnered considerable attention as an exceptional 1D element due to its natural abundance, environmental friendliness, recyclability, structural uniqueness, facile modification, and dimensional stability. Recent advances and future outlooks of nanocellulose as a green material for energy storage systems are described, with a focus on its application in supercapacitors, lithium-ion batteries (LIBs), and post-LIBs. Nanocellulose is typically classified as cellulose nanofibril (CNF), cellulose nanocrystal (CNC), and bacterial cellulose (BC). The unusual 1D structure and chemical functionalities of nanocellulose bring unprecedented benefits to the fabrication and performance of energy storage materials and systems, which lie far beyond those achievable with conventional synthetic materials. It is believed that this progress report can stimulate research interests in nanocellulose as a promising material, eventually widening material horizons for the development of next-generation energy storage systems, that will lead us closer to so-called Battery-of-Things (BoT) era.

forthcoming smart/ubiquitous energy era, which will find the widespread popularity of flexible/wearable electronics, electric vehicles (EVs) and grid-scale ESSs, will necessitate rechargeable power sources to play a more significant role as a key-enabling technology, underscoring the urgency and importance of power source advancement.^[6,7] It is anticipated that rechargeable energy storage systems will incessantly move in the direction of acquiring high energy/power densities, long charge/discharge cycle life, high operating voltages, safety robustness, and cost competitiveness, along with flexibility, miniaturization, and form factors.^[8–11] Conventional energy storage systems are composed of cathodes, anodes, electrolytes, and separator membranes, which are generally based on inorganic/metal compounds, carbonaceous substances and petroleum-derived hydrocarbon chemicals. These traditional materials, however, may have difficulties fulfilling the ever-increasing requirements of the energy storage systems, thus pushing us to search for new chemistries and materials far beyond conventional approaches.

1. Introduction

The remarkable progress in portable electronics achieved during the past decades has undoubtedly been driven by rechargeable energy storage systems (ESSs) such as lithium-ion batteries (LIBs), supercapacitors, and others.^[1–5] The

Among numerous material candidates explored to date, nanocellulose has recently garnered considerable attention as an exceptional 1D element for energy storage systems due to its structural uniqueness, superb properties, natural abundance, and environmental benignity.^[12–17] The rapidly growing research interest in nanocellulose for energy storage systems is witnessed by the annual evolution of the number of published research articles in this field (Figure S1, Supporting Information). Nanocellulose can be exploited in the form of the core element for electrodes, electrolytes, and separator membranes. The unusual 1D structure (typically, a few nanometers in width and several micrometers in length) and the chemical functionalities of nanocellulose are difficult to attain with traditional synthetic materials. As a consequence, nanocellulose has been brought unprecedented benefits to the fabrication and performance of energy storage materials and systems, eventually enabling exceptional improvements in electrochemical performance (such as energy/power densities, rate capability, and long-term cyclability), mechanical flexibility and design diversity that lie far beyond those attainable with conventional synthetic materials.

Herein, stimulated by this increasing research popularity of nanocellulose, we describe recent advances and future outlook

Dr. J.-H. Kim, D. Lee, Y.-H. Lee, Prof. S.-Y. Lee
Department of Energy Engineering
School of Energy and Chemical Engineering
Ulsan National Institute of Science and Technology (UNIST)
Ulsan 44919, Republic of Korea
E-mail: syleek@unist.ac.kr

Prof. W. Chen
Key Laboratory of Bio-Based Material Science and Technology
Ministry of Education
Northeast Forestry University
Harbin 150040, P. R. China
E-mail: chenwenshuai@nefu.edu.cn

The ORCID identification number(s) for the author(s) of this article can be found under <https://doi.org/10.1002/adma.201804826>.

DOI: 10.1002/adma.201804826

of nanocellulose as a green material opportunity for energy storage systems, with a focus on its superiority over traditional synthetic materials. This progress report starts with a brief description of the multihierarchical structures of wood and the structure/characteristics of nanocellulose. Then, the application of nanocellulose is systematically discussed as a function of target energy storage systems, including supercapacitors, LIBs, and post-LIBs (such as lithium–sulfur (Li–S) batteries, sodium-ion batteries (SIBs), and metal–air batteries). An overview of nanocellulose for potential use in energy storage systems is schematically depicted in **Figure 1**. A particular attention is devoted to the beneficial roles of nanocellulose in the component fabrication, electrochemical performance, safety, flexibility, and form factors of the energy storage systems. We envision that this progress report holds a promise as useful guidance and insightful information for design and fabrication of nanocellulose-based energy storage materials and systems.

2. Overview of Nanocellulose

2.1. Hierarchical Structures of Wood

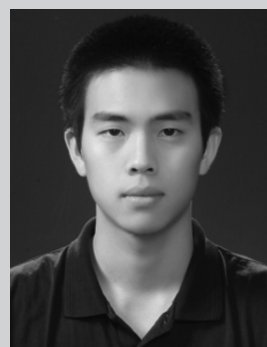
Wood, which is a main source of nanocellulose, naturally has a hierarchical structure, which ranges multiple orders of magnitude in dimensions, contributing different functionalities at each size scale (**Figure 2**). Wood is ≈40–45% of cellulose by weight,^[18] depending on the species. Cellulose is the most naturally abundant organic polymer on Earth and has an annual production, which is estimated to be larger than 7.5×10^{10} tons.^[19] Cellulose is a linear homopolymer of β -1,4-linked anhydro-D-glucose units.^[13,20] The internal hydrogen bonding formed between the hydroxyl groups and oxygens of neighboring molecules contributes to the linkage stability, leading to the linear configuration of the cellulose chain. The intermolecular hydrogen bonds and Van der Waals interaction between adjacent molecules facilitate the parallel stacking of cellulose chains with dimensions of a few Angstroms, which in turn are formed into elementary fibrils with a width of ≈2–5 nm and a length of over 2 μm .^[21,22] The elementary fibrils have both crystalline and amorphous regions. Within the wood cell walls, the elementary fibrils are arranged in parallel and further assembled into nanofibril aggregates with a width of 10–30 nm, which are usually recognized as microfibrils. The microfibrils are further packed and thus form the multilayer structure of wood cell walls and eventually support the body of trees.^[23,24] The aforementioned nanosized cellulose fibrils can be recognized as nanocellulose synthesized by trees. Except trees, nanocellulose can also be produced from/by other resources such as algae, tunicate and bacteria.

2.2. Structure and Characteristics of Nanocellulose

Numerous approaches have been reported to produce nanocellulose with different structures and surface chemistry activities. Based on its preparation, structure, and characteristics, nanocellulose can be classified as cellulose nanofibril (CNF), cellulose nanocrystal (CNC), and bacterial cellulose (BC).



Jung-Hwan Kim received his B.S. degree in chemical engineering from Kangwon National University in 2013. He received his Ph.D. in energy engineering from Ulsan National Institute of Science and Technology (UNIST) in 2018 under the supervision of Professor Sang-Young Lee. His research interests include the design and synthesis of nanocellulose-based paper batteries, nanostructured multi-functional separator membranes, and printed batteries.



Donggue Lee received his B.S. in material science and engineering from Incheon National University in 2014. He is currently an M.S.–Ph.D. integrated course student under the supervision of Prof. Sang-Young Lee. His research interests have focused on the nanoarchitecture with cellulosic materials for advanced rechargeable batteries.



Sang-Young Lee is a professor and a head of School of Energy and Chemical Engineering at UNIST, Republic of Korea. He received a B.A. in chemical engineering from Seoul National University in 1991, M.S., and Ph.D. in chemical engineering from KAIST in 1993 and 1997. He served as a postdoctoral fellow at Max-Planck Institute for Polymer Research from 2001 to 2002. Before joining UNIST, he worked at Batteries R&D, LG Chem as a principal research scientist. His research interests include cellulose-based paper batteries, printed power sources, flexible/wearable batteries, advanced separator membranes, and polymer electrolytes.

2.2.1. Cellulose Nanofibril

Several mechanical apparatuses, including grinders, high-pressure homogenizers, high-intensity ultrasonicators, high-speed blenders, and twin-screw extruders, have been used for the nanofibrillation of cellulose pulps, which are produced from a variety of cellulose resources such as wood, bamboo, crop straw, and potato tuber.^[13,17,25] These methods generate high shear and impact forces that allow mechanical cleavage along the longitudinal direction of the cellulose microfibrillar structure, thereby

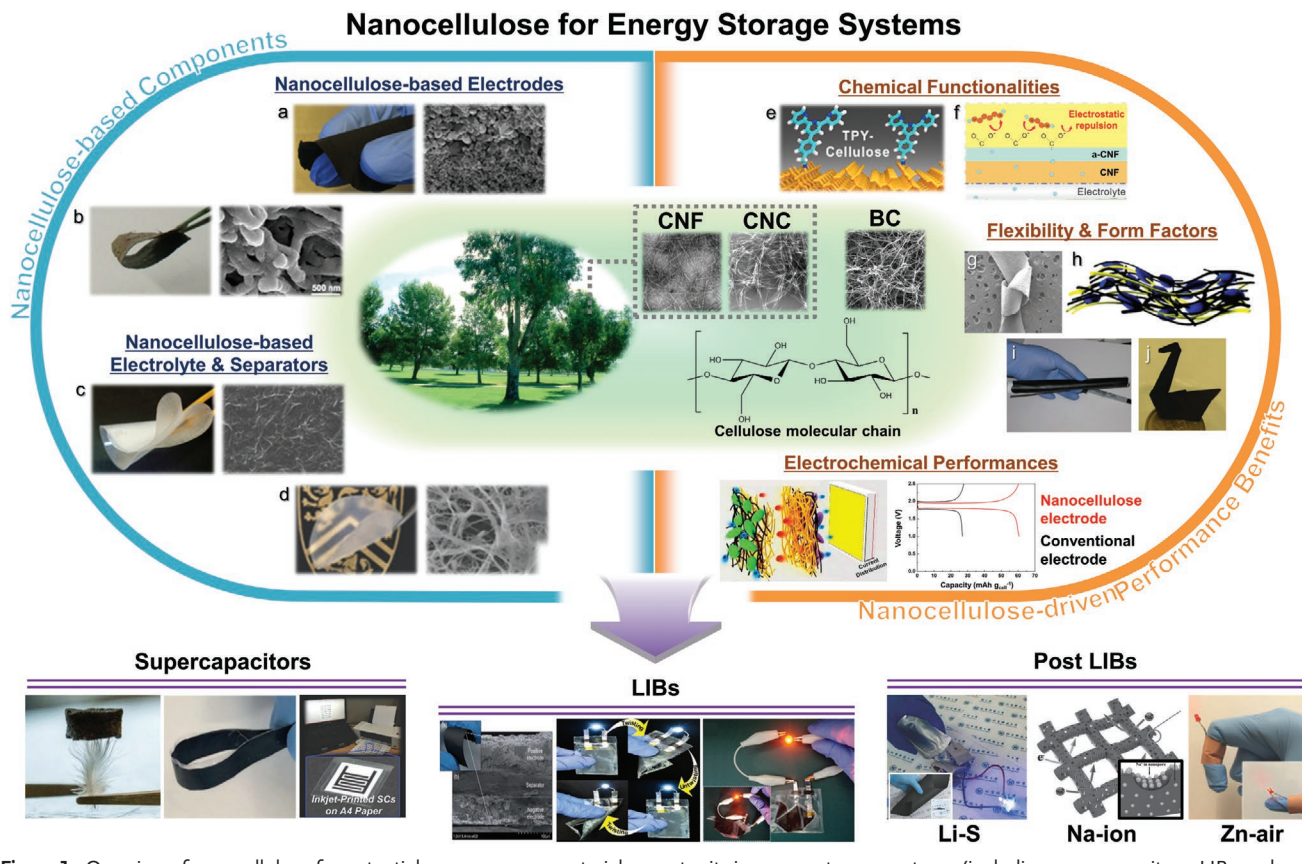


Figure 1. Overview of nanocellulose for potential use as a green material opportunity in energy storage systems (including supercapacitors, LIBs and post-LIBs). TEM image of CNF: Reproduced with permission.^[54] Copyright 2014, Wiley-VCH. TEM image of CNC: Reproduced with permission.^[115] Copyright 2017, Elsevier. SEM image of BC: Reproduced with permission.^[48] Copyright 2017, Wiley-VCH. Photographs and SEM images of “Cellulose-based electrodes”: a) Reproduced with permission.^[116] Copyright 2013, Elsevier. b) Reproduced with permission.^[71] Copyright 2013, Elsevier. Photographs and SEM images of “Cellulose-based electrolyte & separators”: c) Reproduced with permission.^[84] Copyright 2011, Elsevier. d) Reproduced with permission.^[113] Copyright 2016, Royal Society of Chemistry. Illustrations of “Chemical functionalities”: e) Reproduced with permission.^[90] Copyright 2016, American Chemical Society. f) Reproduced with permission.^[96] Copyright 2018, Royal Society of Chemistry. SEM image, illustrations, and photographs of “Flexibility and form factors”: g) Reproduced with permission.^[73] Copyright 2014, American Chemical Society. h) Reproduced with permission.^[74] Copyright 2015, Wiley-VCH. i) Reproduced with permission.^[57] Copyright 2009, National Academy of Sciences. j) Reproduced with permission.^[117] Copyright 2016, Wiley-VCH. Illustrations of “Electrochemical performances”: Reproduced with permission.^[73] Copyright 2014, American Chemical Society. Photographs of “Supercapacitors”: (From left to right) Reproduced with permission.^[49] Copyright 2015, Wiley-VCH. Reproduced with permission.^[118] Copyright 2017, Royal Society of Chemistry. Reproduced with permission.^[56] Copyright 2016, Royal Society of Chemistry. SEM image and photographs of “LIBs”: (From left to right) Reproduced with permission.^[72] Copyright 2013, Royal Society of Chemistry. Reproduced with permission.^[73] Copyright 2014, American Chemical Society. Reproduced with permission.^[74] Copyright 2015, Wiley-VCH. Photographs and illustrations of “Post LIBs”: (From left to right) Reproduced with permission.^[94] Copyright 2017, Wiley-VCH. Reproduced with permission.^[113] Copyright 2016, Royal Society of Chemistry.

resulting in the extraction of long and entangled CNF. Generally, CNF has high aspect ratio and exhibits web-like entangled morphologies. The structure and nanofibrillation degree of CNF are highly affected by the cellulose source, mechanical/chemical/enzyme pretreatment, nanofibrillation equipment, and nanofibrillation processing times/repeating cycles.^[17,26] The unique structures and properties of CNF, including the high aspect ratio, web-like entangled structures, and outstanding mechanical properties, have beneficially contributed to the realization of high-performance energy storage systems. Further details will be described in the subsequent sections.

2.2.2. Cellulose Nanocrystal

CNC generally refers to a kind of nanocellulose obtained by strong acid hydrolysis methods.^[17,26] During hydrolysis process,

the paracrystalline or disordered parts of cellulose are hydrolyzed and dissolved in the acid solution, while the crystalline parts show a chemical resistance to acid and remain intact. Consequently, the cellulose fibrils are transversely cleaved, producing the short CNC with relatively high crystallinity. The structure (such as width, length, aspect ratio, and degree of aggregation) and surface chemistry of CNC are generally determined by the cellulose source, nature of the acid, concentration of the acid, acid to pulp ratio, and hydrolysis conditions, as well as the subsequent nanofibrillation treatment. During the sulfuric-acid-driven hydrolysis process, sulfuric acid also reacts with the hydroxyl groups at the surface of cellulose to generate charged surface sulfate esters that can promote the isolation of individual CNC and the uniform dispersion of the CNC in water. Generally, a wood CNC is 3–5 nm in width and 100–200 nm in length, while a cotton CNC is 5–10 nm in width

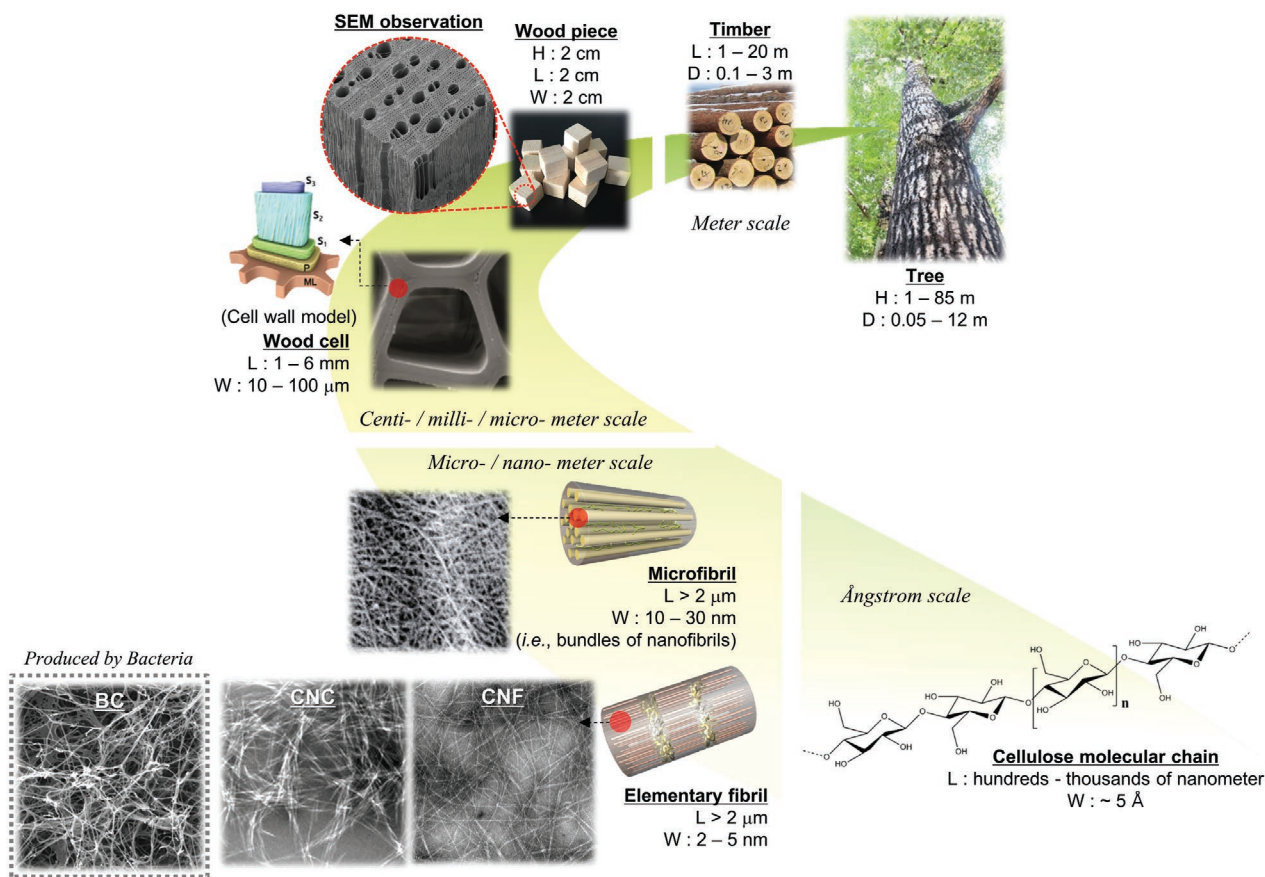


Figure 2. Schematic representation illustrating the hierarchical structure of wood. Multiple orders of magnitude in dimensions and chemical structures are depicted. SEM image of wood piece: Reproduced with permission.^[119] Copyright 2012, Scientia Silvae Sinicae. SEM image of wood cell: Reproduced with permission.^[120] Copyright 2018, Springer Nature. SEM image of microfibril: Reproduced with permission.^[121] Copyright 2009, Springer. TEM image of CNF: Reproduced with permission.^[54] Copyright 2014, Wiley-VCH. TEM image of CNC: Reproduced with permission.^[115] Copyright 2017, Elsevier. SEM image of BC: Reproduced with permission.^[48] Copyright 2017, Wiley-VCH.

and 100–300 nm in length.^[12] The CNC with high specific surface area can be easily dispersed in water and form a chiral nematic organization, thereby enabling the facile integration with electrode active materials and the formation of novel structural carbon materials. Additional details will be described in the later sections.

2.2.3. Bacterial Cellulose

BC is a kind of nanocellulose generated by several species of bacteria belonging to the genera *Acetobacter*, *Rhizobium*, *Agrobacterium*, and *Sarcina*.^[27–29] *Acetobacter xylinum* is known as the most efficient producer. This organism can generate sugar, glucose, glycerol, or other organic substrates and convert them into BC. Thus, BC is recognized as a biotechnology product. The synthesis of cellulose in *Acetobacter xylinum* is allowed between the cytoplasma membrane and outer membrane by a cellulose-synthesizing complex, which is in close association with pores on the surface of the bacterium.^[30] The obtained cellulose leaves the pores as fibrils and gets assembled together with a number of synthesized fibrils into a ribbon-like crystalline cellulose. Different from wood CNF, BC is pure cellulose

free of other components such as hemicellulose. It exhibits a high degree of polymerization (up to 8000) and forms a 3D network of interconnected nanofibers without any preferential orientation.^[31,32] Due to its unusual characteristics mentioned above, BC has recently gained considerable interest for use in various energy storage systems.

3. Overview of Nanocellulose for Use in Energy Storage Systems

Nanocellulose has been investigated as a promising green alternative to conventional energy storage materials. Note that the unusual 1D structure and chemical diversity of nanocellulose provide exceptional performance improvements, which are difficult to achieve with traditional synthetic materials, to energy storage materials and systems. Table S1 (Supporting Information) summarizes representative examples of nanocellulose and its derivatives for use in various energy storage systems, with an attention to components, the preparation and performance of the energy storage systems. More details are systematically described in the subsequent sections.

4. Nanocellulose for Supercapacitors

The electrochemical performance of supercapacitors is usually expressed in terms of specific capacitance, energy density (energy stored per unit mass/volume/area/length) and power density (power generated per unit mass/volume/area/length).^[33] Depending on the charge/discharge mechanism, supercapacitors can be largely classified as two different systems: i) electrical double-layer capacitors, in which electrochemical energy is stored by the adsorption/desorption of ions, and ii) pseudocapacitors based on redox reactions. As shown in Figure 3a, nanocellulose has been exploited as an electrode binder that holds electroactive materials. The nanocellulose-derived films/aerogels have been investigated as structural substrates that can

accommodate subsequent deposition of electrically conductive or electroactive materials to produce electrode sheets and supercapacitor systems. In addition, nanocellulose has been utilized as a precursor for carbon materials (obtained via pyrolysis). Representative examples of nanocellulose-based supercapacitors and their electrochemical/mechanical superiorities are summarized in Table S2 (Supporting Information).

4.1. Nanocellulose-Based Electrode Binders

Nanocellulose has been integrated with various electroactive materials^[34–39] as an alternative electrode binder to replace conventional synthetic polymer-based ones. Notably, CNF, due to

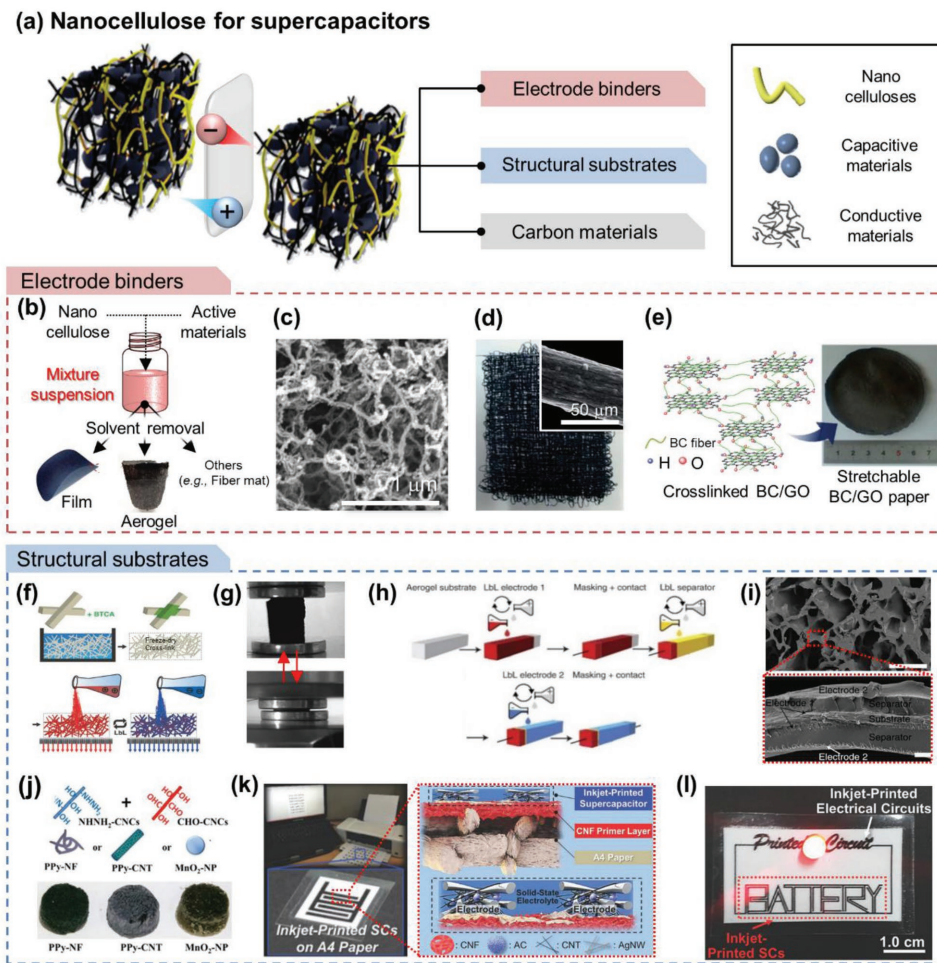


Figure 3. Nanocellulose-based electrode binders and substrates for supercapacitors. a) A conceptual illustration of nanocellulose for use in supercapacitor electrodes. b) A schematic of fabrication process of nanocellulose-based composite electrodes. c) SEM image of a CNF/MWCNT hybrid aerogel obtained by supercritical CO₂ drying. d) Reproduced with permission.^[34] Copyright 2013, the Royal Society of Chemistry. e) A schematic of crosslinked BC/GO and photograph of composite paper. Reproduced with permission.^[39] Copyright 2015, the Royal Society of Chemistry. f) An illustration of PEI/SWCNT on a crosslinked CNF aerogel fabricated through LbL assembly. g) Photographs of reversibly compressible (PEI/SWCNT)/CNF aerogel. f,g) Reproduced with permission.^[40] Copyright 2013, Wiley-VCH. h) A schematic of (PEI/CNT)/CNF aerogel-based 3D supercapacitor fabricated through LbL assembly. i) Cross-sectional SEM images of a (PEI/CNT)/CNF aerogel. h,i) Reproduced with permission.^[41] Copyright 2015, Springer Nature. j) A schematic of aerogel components and photographs of resultant hybrid aerogels. Reproduced with permission.^[49] Copyright 2015, Wiley-VCH. k) A photograph of inkjet-printed SCs and illustration of inkjet-printed SCs. l) Photograph of the inkjet-printed, letter-shaped SC (marked by a red box). k,l) Reproduced with permission.^[56] Copyright 2016, the Royal Society of Chemistry.

its unique 1D fibrous feature and mechanical compliance, has frequently been explored for this purpose. A variety of nanocellulose-based composite electrodes have been produced through the solvent removal process (i.e., vacuum filtration, supercritical drying, solvent exchange, and so on) using CNF/carbon mixture suspensions (Figure 3b). A CNF/multiwalled carbon nanotube (MWCNT) hybrid aerogel^[34] with uniform morphology was obtained by supercritical carbon dioxide (CO_2) drying (Figure 3c). A hybrid aerogel was used for a symmetric, flexible and all-solid-state supercapacitor. Shao and co-workers^[35] prepared a CNF/reduced graphene oxide (rGO) hybrid aerogel, in which the CNF acted as a nanospacer for rGO. In this CNF/rGO hydrogel, the CNF effectively reduced the π - π stacking interactions of rGO and prevented the aggregation of rGOs. CNF/single-walled carbon nanotube (SWCNT) mats (Figure 3d) were produced through extrusion of a CNF/SWCNT suspension in an ethanol coagulation bath followed by drying under restricted conditions.^[36] The CNF/SWCNT mats showed a well-developed porous structure with the SWCNTs preferentially oriented along the extrusion direction. The CNF suppressed the aggregation of the SWCNTs, thus facilitating electron transport along the longitudinal direction of the fibers. The as-prepared non-woven mat-type supercapacitor exhibited good electrochemical properties, outstanding customizability and damage resilience, demonstrating their potential use as a wearable power source. A 2D composite paper composed of crosslinked BC/GO was fabricated through the intermolecular esterification of mixture components (Figure 3e).^[39] The composite paper showed a good stretchability with tensile strength of 18.5 MPa and elongation at break of 24%.

4.2. Nanocellulose-Based Structural Substrates

Nanocellulose-derived films/aerogels have been used as structural substrates that can accommodate subsequent deposition of electrically conductive or electroactive materials to develop flexible electrodes and supercapacitors.^[40–49] Hamed et al.^[40] reported layer-by-layer (LbL) assembly of SWCNTs on a cross-linked CNF aerogel (Figure 3f), creating a composite aerogel with porosity close to 99%, as well as yielding high strength and structural integrity in water. The CNF aerogel-based supercapacitor showed exceptional compressibility and reliable electrode capacitance (Figure 3g). They also developed a compressible, 3D supercapacitor through the LbL self-assembly of multi-layered films on the surface of an open-cell aerogel substrate based on CNF (Figure 3h).^[41] A negatively charged, cross-linked CNF aerogel was exploited as a substrate, and the negative and positive electrodes were coated onto the aerogel. An anionic ($-\text{COOH}$ -functionalized) SWCNT layer was combined with a cationic polyethyleneimine (PEI) layer to produce electrode layers and a layer of PEI/polyacrylic acid was employed as a separator membrane and electrolyte. The LbL method successfully enabled ultrathin and well-interconnected nanoporous coating layers throughout the whole CNF network (Figure 3i), thereby facilitating the electrochemical activity of the active materials. The cell capacitance of the resultant 3D supercapacitor was maintained after the repeated compression for 400 cycles, with a capacitance of 25 F g^{-1} based on active mass. The CNT-coated

cellulose fibers were fabricated as an electroconductive support, in which the cellulose fibers served as a support with a large surface area and acted as an interior electrolyte reservoir.^[50] In the CNT-coated cellulose fiber support, the electrolyte easily adsorbed on the cellulose fibers and was therefore ready to diffuse into the electrode active materials.

ECPs, including polypyrrole (PPy), polyaniline (PANI), and poly(3,4-ethylene dioxythiophene) (PEDOT), have been considered as a promising pseudocapacitive electrode material for supercapacitors. The hydroxyl groups on the cellulose surface allow for strong inter- and intramolecular hydrogen bonds with ECPs, thus, enabling the nanocellulose to act as an ideal substrate for nonmetal-based electrode materials.^[51] A thin ECP layer on the nanocellulose scaffold increases the specific capacitance of the electrode via the combination of Faradic reactions and a large active surface area and reduces the strain inducing volume changes during charge/discharge cycling. Representative examples include flexible and porous CNF/PPy electrodes.^[42,47,52,53] Pyrrole was chemically polymerized by iron(III) chloride to form thin, uniform coating layers of PPy on CNF substrates. The resultant CNF/PPy composite electrodes exhibited more rapid oxidation/reduction reactions and higher capacitances than those of thick PPy films.^[42] Wang et al. introduced quaternary amine groups onto the CNF surface to prepare cationically charged CNF (c-CNF).^[43] The polymerization of pyrrole on the c-CNF produced c-CNF/PPy composites with an evenly compactly morphology.

In addition to CNF, BC and CNC were also combined with ECPs to fabricate nanocellulose-based supercapacitor electrodes. BC/PANI composites were synthesized via the polymerization of aniline on BC substrates.^[44] However, these composite electrodes were brittle, resulting in a poor mechanical flexibility. To resolve this problem, a MWCNT-coated BC substrate was prepared, and PANI was then electrodeposited onto the substrate, thus, producing flexible and lightweight PANI/MWCNT/BC electrodes.^[45]

CNC has been widely explored as a substrate due to their excellent mechanical strength and dimensional characteristics. Walsh and co-workers^[46] reported a CNC/PPy composite synthesized through electrochemical deposition of a thin PPy layer onto anionically charged CNCs (a-CNCs). The a-CNCs acted as a kind of counterion to balance the positive charges on the polymer backbone during the electrodeposition, resulting in a highly porous composite film. The CNC/PPy composite electrodes provided a higher capacitance (336 F g^{-1}) than the conventional PPy (i.e., doped with Cl^- ions) (258 F g^{-1}).

The CNC composite electrodes, however, tend to be mechanically weak^[54] and are easily broken upon external deformation. To overcome these shortcomings, an approach based on crosslinked CNC aerogels was suggested.^[49,55] The CNC aerogels were fabricated based on the chemical crosslinking of aldehyde-modified CNCs and hydrazide-modified CNCs. These CNC aerogels acted as universal substrates for a variety of capacitive materials, including PPy nanofibers, PPy-coated CNTs and spherical manganese dioxide nanoparticles during the aerogel assembly (Figure 3j). Notably, the capacitive materials interacted with the cross-linked CNCs via hydrogen bonding and/or nonpolar interactions to produce gel-like

structures, which were eventually transformed to hybrid aerogels by freeze drying/supercritical drying. The obtained aerogels showed a high capacitance retention of over 94% after 2000 cycles at 0.1 mA cm^{-2} .

Lee and co-workers^[56] reported all-inkjet-printed, solid-state flexible supercapacitors directly fabricated on commercial A4 paper. The CNF-mediated nanomat, which was inkjet-printed as a primer layer, played a viable role in enabling the inkjet printing of electrodes and electrolytes (Figure 3k). The resultant inkjet-printed supercapacitors showed a good mechanical flexibility, exceptional form factors and reliable electrochemical performance (Figure 3l).

Apart from nanocellulose-derived paper, conventional paper has been investigated as a substrate for electrodes.^[57,58] Cui and co-workers^[57] reported a simple way to fabricate conductive paper sheet by coating CNT inks on commercial photocopy paper. The intrinsic attributes of paper, including facile adsorption of solvents and strong binding with nanomaterials, allowed for the fabrication of supercapacitors based on CNT-coated conductive paper.

4.3. Nanocellulose-Derived Carbonaceous Materials

Most carbonaceous materials for use in energy storage systems are based on fossil fuels as precursors.^[59] Recently, nanocellulose has drawn substantial attention as an environmentally friendly precursor for carbonaceous materials. The high-temperature pyrolysis of nanocellulose under an inert atmosphere converts nanocellulose into conductive carbon materials. The nanocellulose-derived carbons can be classified as porous carbon, heteroatom-doped carbon and carbon composites (Figure 4a).

CNF and BC have often been used as building elements to prepare porous carbon aerogels.^[60–67] The activation of carbon aerogels by catalysts such as potassium hydroxide (KOH)^[60,67] or potassium citrate^[68] is known to effectively improve the specific surface areas for charge accommodation, thus, increasing the specific capacitance of the resultant carbon aerogels. Fan and co-workers^[60] introduced KOH to facilitate the crosslinking reaction of BC and to generate macropores during the carbonization process. The obtained carbon aerogels had a

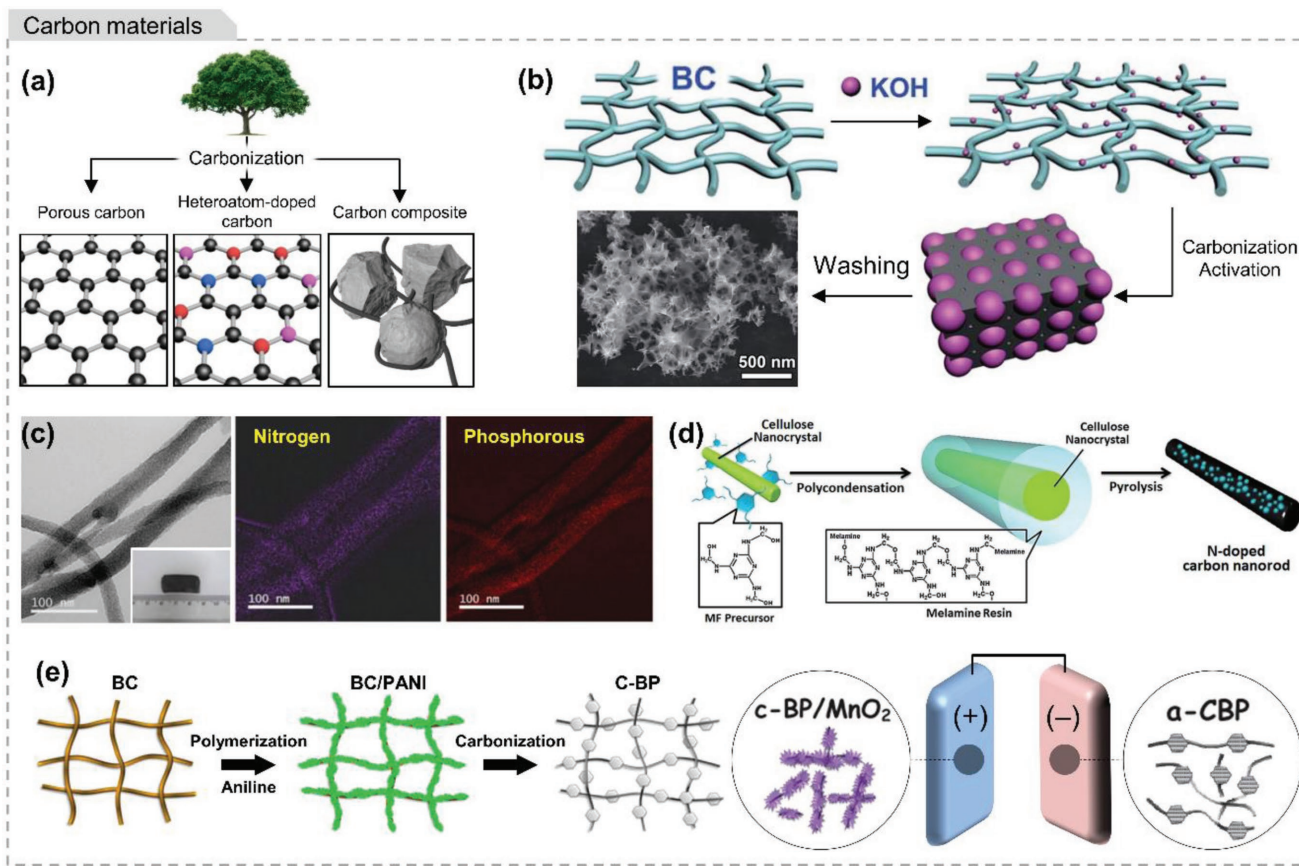


Figure 4. Nanocellulose-derived carbonaceous materials for supercapacitors. a) A conceptual illustration of cellulose-derived carbonaceous materials: porous carbon, heteroatom-doped carbon, and carbon composites. b) A schematic illustration depicting the synthetic procedure of carbon aerogels with 3D interconnected honeycomb-like hierarchical network structure. Reproduced with permission.^[60] Copyright 2016, the Royal Society of Chemistry. c) Energy-filtered TEM images of N,P-doped BC and elemental mapping images of N and P. Reproduced with permission.^[63] Copyright 2014, Wiley-VCH. d) A schematic representation of the two-step synthesis of N-doped carbon nanorods from melamine-formaldehyde (MF)-coated CNC. Reproduced with permission.^[65] Copyright 2015, the Royal Society of Chemistry. e) A schematic representation of an asymmetric supercapacitor based on MnO₂-coated pyrolyzed BC (c-BP) as a positive electrode and nitrogen-doped c-BP (a-CBP) as a negative electrode. Reproduced with permission.^[67] Copyright 2014, Wiley-VCH.

3D interconnected honeycomb-like hierarchical network structure (Figure 4b).

Oh and co-workers^[61] developed lignin-based flexible aerogels and carbon aerogels. Lignins have drawn significant attention, because they have three different phenolic alcohol monomers linked together via C–C or C–O–C linkages to form 3D polymer networks and show a lattice structure comprised of aromatic carbons. However, lignin-resorcinol-formaldehyde (LRF) aerogels and their carbon aerogels are mechanically brittle. BC was introduced to address this issue. The BC was added into the LRF solution, and the mixture was subjected to a polycondensation reaction, producing BC/LRF hydrogels. After CO₂ supercritical drying and catalyst-free carbonization, the BC/LRF aerogels and their carbon aerogels were obtained. The aerogel-based electrodes showed an outstanding cycling performance (98% capacity retention after 10 000 cycles). Recently, Hu and co-workers^[62] proposed an all-wood-structured, biodegradable, and low tortuosity supercapacitor assembled with an activated wood carbon anode, wood membrane separator, and MnO₂/wood carbon cathode. The all-wood structure with straightforwardly formed channels contributed to the high power density as well as high energy density.

The structural engineering of carbon materials by substitution of some atoms with heteroatoms, including nitrogen (N), phosphorus (P), boron (B), sulfur (S), iodine (I) and others, is known to be effectively tailor their electron-donor properties.^[63] As a representative example, plenty of nitrogen-doped carbon materials have been produced by posttreatment with ammonia gas or carbonization of nitrogen-enriched precursors, which often involve hazardous operating conditions or time-consuming synthetic processes. As a facile way to resolve this issue, an ammonia solution was used as a reaction precursor. A nitrogen-doped, 3D carbon nanofiber network was prepared from the pyrolyzed BC.^[64] To introduce nitrogen into the pyrolyzed BC, a hydrothermal reaction with an aqueous ammonia solution was conducted. A similar approach was reported with heteroatom-containing substances that were added as a dopant.^[63] BC slices were immersed in H₃PO₄, NH₄H₂PO₄, and H₃BO₃/H₃PO₄ aqueous solutions. The abundant functional groups of BC readily enabled doping with phosphorus, boron/phosphorus, and nitrogen/phosphorus groups. After drying and carbonization, the 3D heteroatom-doped carbon nanofiber networks were obtained (Figure 4c). CNC has been exploited as a carbon source as well as a template for the controlled growth of a nitrogen precursor to generate melamine-formaldehyde (MF)-coated CNC.^[65] The MF precursor/CNC mixture was pyrolyzed to fabricate N-doped carbon materials with micro-, meso-, and macropores (Figure 4d).

In addition to the heteroatom doping approach described above, the synthesis of pseudocapacitive materials based on nanocellulose-derived carbon materials was suggested.^[66,67] An asymmetric supercapacitor was fabricated using the MnO₂-coated pyrolyzed BC (c-BP) as a positive electrode and the nitrogen-doped c-BP (a-CBP) as a negative electrode (Figure 4e).^[67] The BC was employed as a raw material to fabricate a 3D nanofibrous carbon network of c-BP via annealing at 1000 °C. Then, the MnO₂-coated c-BP was fabricated using KMnO₄/K₂SO₄ aqueous solution via hydrothermal reaction.

5. Nanocellulose for LIBs

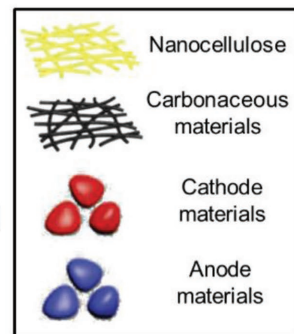
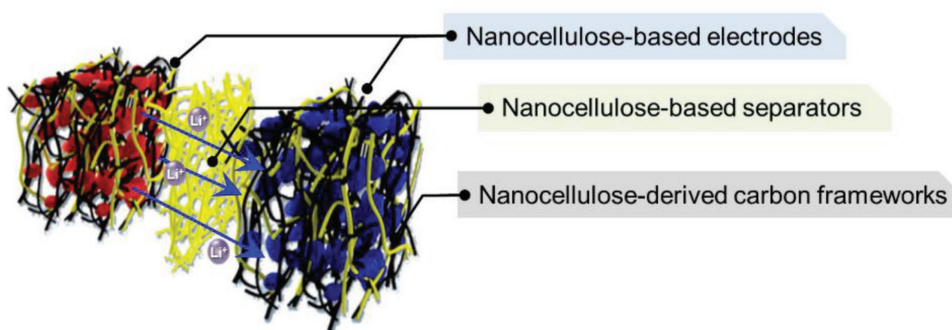
Since the commercialization of LIBs in 1991, LIBs have garnered a great deal of attention in a vast variety of application fields due to their high operation voltage, high energy density, long cycle life, negligible memory effect, and low self-discharge. As a new material approach to fuel the sustainable growth of LIBs, nanocellulose has been investigated for potential use in electrode components (specifically, electrode binders (or substrates) and precursors for carbon materials) and as an additive of solid composite electrolytes and porous separator membranes. The application of nanocellulose to LIBs is conceptually illustrated in Figure 5a. The structural/electrochemical/mechanical characteristics of the nanocellulose-based LIBs are summarized in Table S3 (Supporting Information).

5.1. Nanocellulose-Based Electrodes and All-Paper Batteries

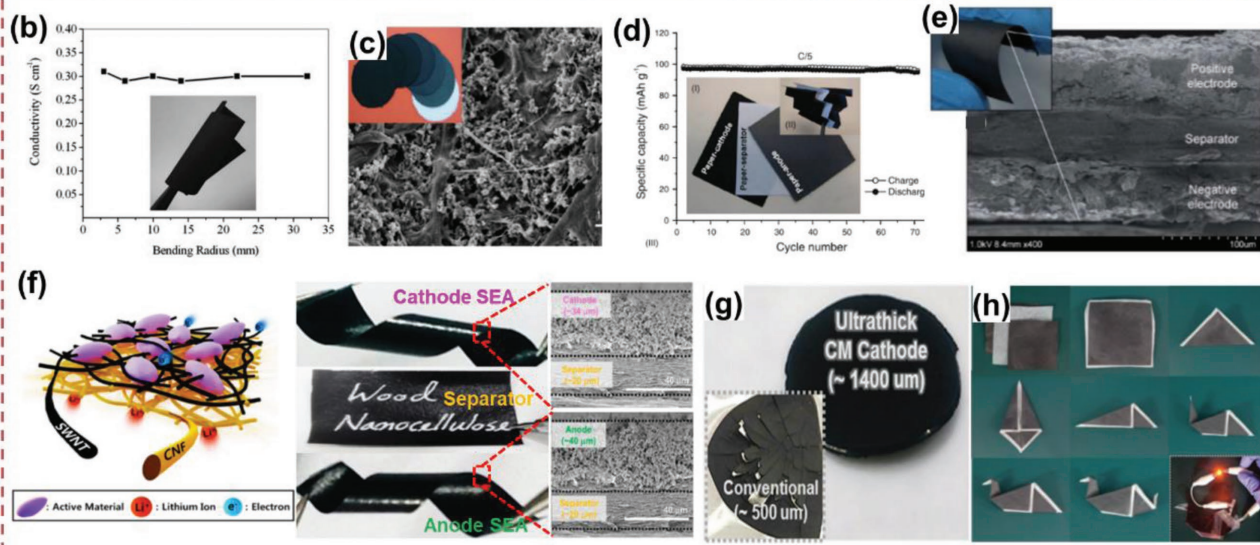
Driven by their excellent mechanical compliance and large aspect ratio, CNF can be used as an alternative electrode binder to current state-of-the-art synthetic polymer binders.^[69–74] Conventional LIB electrodes consist of active materials, electronic conductive additives (such as carbon black), and polymeric binders on top of heavy metallic current collectors. As a representative polymer binder of LIB electrodes, polyvinylidene fluoride (PVdF) has most widely been used.^[75,76] However, PVdF requires the use of organic solvents such as N-methyl-2-pyrrolidinone (NMP), that are toxic and demand high-cost/complicated drying units for electrode fabrication processes. Moreover, upon application to flexible power sources, the mechanical properties of PVdF are insufficient to withstand the applied external deformation. Beneventi and co-workers^[69] demonstrated that CNF can be used as a binder for flexible graphite anodes that were fabricated through a water evaporation process. The as-prepared graphite anodes showed well-developed porous structure and maintained good mechanical flexibility (Figure 5b). Jabbour et al.^[70] developed self-standing LiFePO₄ paper cathodes using the CNF as a cathode binder. The paper cathodes were prepared through filtration of an aqueous cathode suspension incorporating LiFePO₄ particles, carbon black, and CNF in different composition ratios. The LiFePO₄/carbon black-embedded fibrous morphology of the composite paper cathode is shown in Figure 5c, in which the inset shows the color change of the composite papers as a function of CNF content. In addition to the LiFePO₄ paper cathodes, graphite paper anodes and paper separators were also fabricated using the vacuum filtration method. A paper cell composed of LiFePO₄ paper cathode, graphite paper anode, and paper separator was fabricated (Figure 5d). The paper cell exhibited a specific capacity of ≈100 mAh g⁻¹ and a stable capacity retention up to 70 cycles. In addition, the components of the paper cell were folded without any mechanical rupture. These results demonstrate the potential applicability of CNF as an alternative electrode binder and the feasibility of all-paper LIBs as a new power source.

Cui and co-workers^[71] reported lightweight, conductive CNF paper coated with a silicon (Si) thin layer and its application as a LIB anode. Si is an appealing alloy-type anode material due to its

(a) Nanocellulose for Li-ion batteries



Nanocellulose-based electrodes and all-paper batteries



Nanocellulose-derived carbon frameworks

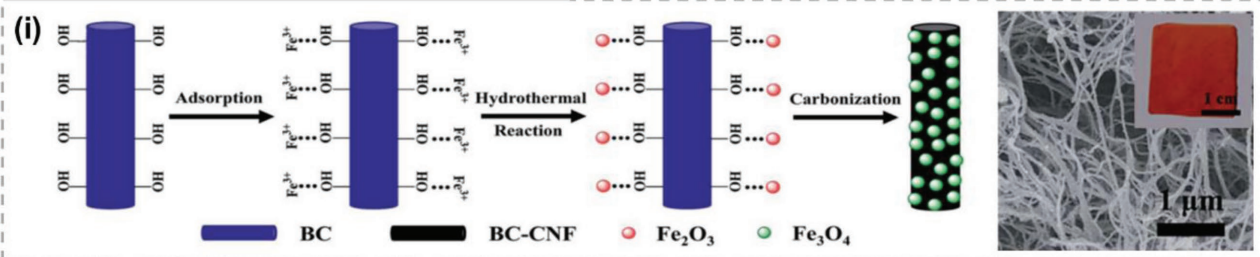


Figure 5. Nanocellulose-based electrodes, all-paper batteries, and carbonaceous materials for LIBs. a) A conceptual illustration depicting application of nanocellulose to LIBs. b) Electronic conductivity of an MFC-graphite anode as a function of bending radius. b) Reproduced with permission.^[69] Copyright 2010, the Royal Society of Chemistry. c) Photograph and SEM image of CNF/LiFePO $_4$ paper cathode. d) Cycling performance of a paper cell. Inset shows the components of the paper cell before/after folding. c,d) Reproduced with permission.^[70] Copyright 2013, Springer. e) SEM image (cross-sectional) of a paper battery. The inset shows its mechanical flexibility. Reproduced with permission.^[72] Copyright 2013, the Royal Society of Chemistry. f) A schematic illustration, photographs and cross-sectional SEM images of flexible LiFePO $_4$ (cathode) and Li x Ti $_5$ O $_{12}$ (anode) SEAs. Reproduced with permission.^[73] Copyright 2014, American Chemical Society. g) Photographs of dimensionally tolerable ultrathick (thickness \approx 1400 μm) CM cathode. Inset shows poor structural stability of a conventional cathode (thickness \approx 500 μm). h) Photographs of origami-folding-based stepwise multifolding procedure for making the paper crane cell and its electrochemical activity. g,h) Reproduced with permission.^[74] Copyright 2015, Wiley-VCH. i) A schematic illustration of the synthetic procedure and SEM image of a Fe $_3$ O $_4$ -carbon nanofiber aerogel derived from BC. Reproduced with permission.^[79] Copyright 2015, the Royal Society of Chemistry.

high specific capacity relative to other materials (4200 mAh g $^{-1}$). The CNT-Si-coated CNF/CNT aerogels were fabricated by a plasma-enhanced CVD (PECVD) method. The conductive

CNF/CNT aerogel conductive paper was physically flexible and could be cut into various sizes and shapes. The discharge capacity retention of the Si-coated CNF paper remained 83%

after 100 charge/discharge cycles. Such stable cyclability of the Si-coated CNF paper was attributed to the CNF/CNT-mediated 3D conductive framework with good mechanical tolerance that acted as a kind of dimensional cushion, and thus, withstood the volume change of the Si active materials during repeated lithiation/delithiation.

All-nanocellulose-based, flexible paper cells were reported by Leijonmarck et al.^[72] Note that CNF was used as both a separator membrane and an electrode binder. The paper battery was made through a traditional paper-making process by sequentially filtrating aqueous anode/separator/cathode suspensions. The cross-sectional SEM image revealed three discrete and tightly adhering layers, which were assigned to the cathode, separator, and anode (Figure 5e). After hundreds of cycles, the paper cell presented a meaningful level of capacity retention. The capacity decay was believed to be a loss of cyclable lithium, plausibly because of parasitic side reactions with water molecules.

Recently, inspired by the 1D structural uniqueness of CNF and CNT, Lee and co-workers^[73] demonstrated separator/electrode assembly (SEA) architecture based on a heterolayered 1D-nanobuilding-element mat (*h*-nanomat). The unitized SEA consisted of a wood CNF-based separator membrane and electrodes comprised of SWCNT-netted electrode active materials without metallic current collector/polymeric binder components. The SEA, a key unit of the *h*-nanomat battery, was fabricated through a facile vacuum-assisted infiltration process. After the electrode suspension introduced on the CNF paper was vacuum-dried, the self-standing and flexible cathode (or anode) SEA was produced (Figure 5f). The current collectors of electrodes are known to allow electron transport toward electrode active materials and act as a dimensional support layer for electrodes. However, heavy metallic foil-based current collectors negatively affect gravimetric capacity of electrodes. In SEAs, removing the metallic current collectors as well as the polymeric binders enabled the loading of a larger amount of electrode active materials, thus leading to a substantial increase in (electrode mass-based) specific capacity. Moreover, the structural uniqueness of SEAs enabled significant improvements in the shape flexibility of the *h*-nanomat cells.

Lee and co-workers^[74] reported hetero-nanonet (HN) paper batteries based on 1D CNF/MWCNT building elements. The HN paper batteries were composed of CNF/MWCNT-intermingled electrodes and a CNF separator. The CNF/MWCNT-based paper electrodes were prepared using a vacuum-assisted infiltration analogous to the typical paper-making process. Because of the flexible characteristics driven by the 1D building elements, a self-standing, ultrathick (thickness ≈1400 μm) CM LiFePO₄ cathode was prepared without impairing its dimensional stability (Figure 5g). By comparison, for the conventional LiFePO₄ cathode fabricated by the conventional slurry coating process, serious concerns with structural integrity were observed at a cathode thickness of ≈500 μm (inset image of Figure 5g). Furthermore, the heteronet-driven mechanical compliance of the paper electrodes, in collaboration with a readily deformable CNF separators, allowed the realization of paper crane batteries through an origami folding technique (Figure 5h).

Nanocellulose-derived carbon materials have been investigated as a low-cost and environmentally benign strategy to

fabricate a 3D porous electrode structures. Pyrolyzed CNF and BC can be directly introduced as conductive carbon frameworks for flexible LIBs.^[77–81] Nano-SnO₂, nano-Ge,^[77] nano-Fe₃O₄,^[79] amorphous Fe₂O₃,^[80] and MoS₂ nanoleaves^[81] were successfully synthesized on nanocellulose-derived carbon frameworks through an in situ growth method for the preparation of flexible anodes (Figure 5i). Recently, inspired by anisotropically aligned channel structure of the natural wood materials, Hu and co-workers^[82,83] fabricated a highly porous, low-tortuosity carbon framework obtained from the direct carbonization of natural wood and explored its potential application as an ultrathick 3D current collector or a Li host material. The conductive carbon framework allowed for the ultrahigh mass loading of active materials and the reliable Li stripping/plating.

5.2. Nanocellulose-Based Solid Composite Electrolytes and Separator Membranes

In conventional LIBs, liquid electrolytes are most widely used due to their high ionic conductivity and well-tailored electrochemical attributes. However, their fluidic characteristics and flammability give rise to undesirable safety problems such as electrolyte leakage and cell combustion/explosion. Such intrinsic limitations of liquid electrolytes force us to search for new alternatives such as gel- and solid-type electrolytes. Among numerous approaches to reach this goal, nanocellulose has been explored as a building element for solid-state electrolytes.^[84–86] Chiappone et al.^[84] reported gel-polymer electrolyte (GPE) membranes composed of CNF (as a mechanical filler) and a methacrylic-based polymer matrix (Figure 6a). A difunctional methacrylic oligomer (1-(butoxy)ethyl methacrylate, BEMA) and monofunctional (poly(ethylene glycol) monomethyl ether methacrylate, PEGMA) polymer were photopolymerized in the presence of CNF. The CNF contributed to improving the tensile strength and the Young's modulus. Even after being swollen in the electrolyte solution, the resultant GPEs showed good dimensional stability and mechanical behavior (inset image of Figure 6a).

The separator membrane of LIBs serves as an electrically insulating layer and provides ion-transport channels. An ideal separator membrane requires well-developed porous structure and strong mechanical/thermal stability. CNF has a high melting point of 260–270 °C compared to most widely used polyolefins and easily forms CNF-mediated 3D porous networks. Intrigued by these unique features, CNF has been investigated as a new material to develop alternative separator membranes beyond commercial polyolefin-based ones.^[87–90] Lee and co-workers^[87,88] pioneered CNF paper-derived separator membranes. The highly interconnected nanoporous structure exhibited an affinity toward the electrolyte and was established between closely piled CNFs. Isopropyl alcohol (IPA) and silica nanoparticles (SiO₂) were introduced as CNF-disassembling agents, while water promoted the dense packing of CNFs (Figure 6b–e). The CNF-disassembling agents allowed for the loose packing of CNFs, thereby promoting the evolution of a highly porous structure. The porous structure was fine-tuned by changing the contents of the CNF-disassembling agents in the CNF suspension. The CNF paper separator showed good

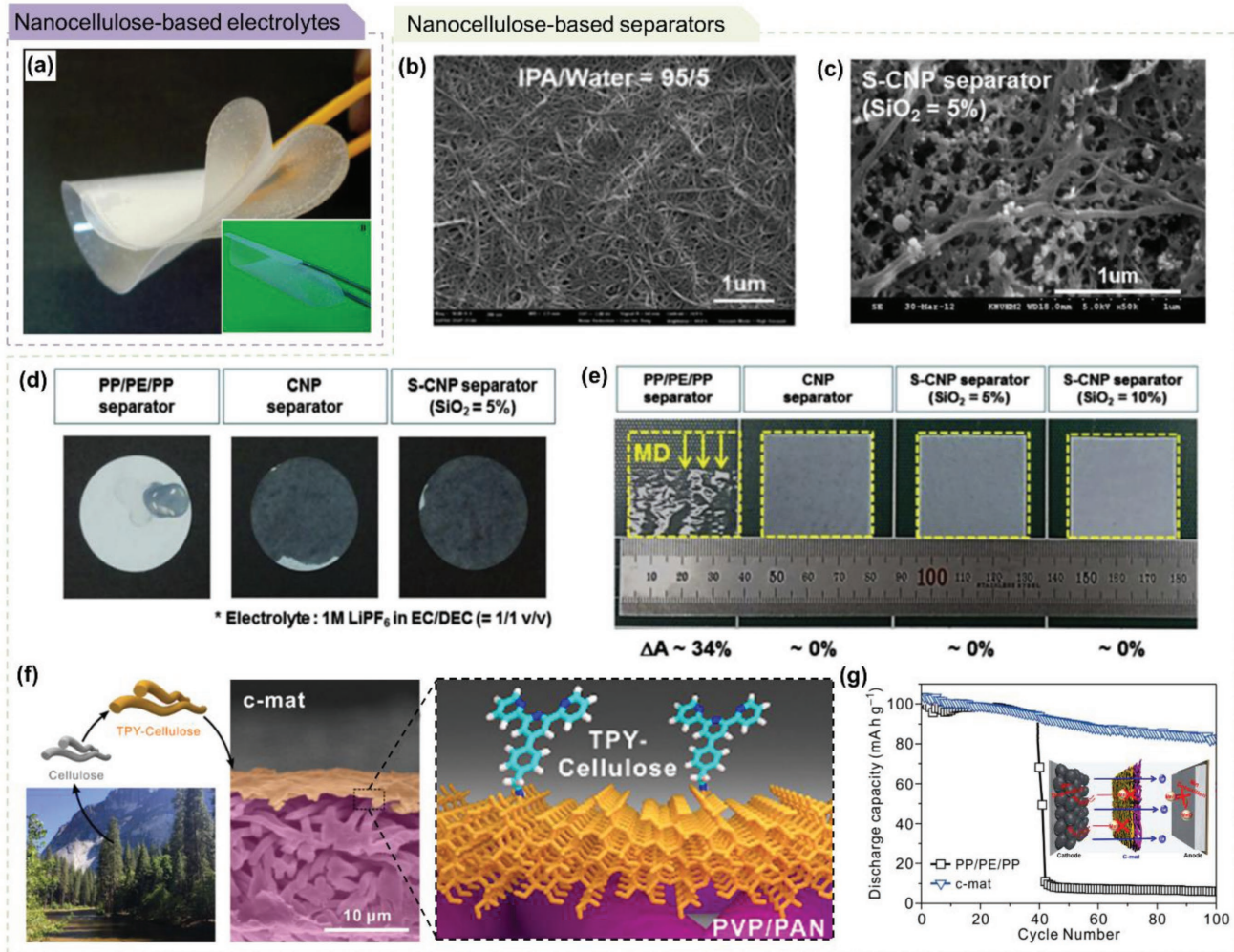


Figure 6. Nanocellulose-based solid composite electrolytes and separators for LIBs. a) Photograph of a GPE membrane composed of CNF (as a mechanical filler) and a methacrylic-based polymer matrix. The inset shows the GPE after absorbing liquid electrolyte for 2 h. Reproduced with permission.^[84] Copyright 2011, Elsevier. b) SEM image of CNF separator [IPA/water = 95/5 (v/v)]. Reproduced with permission.^[87] Copyright 2012, the Royal Society of Chemistry. c) SEM image of S-CNF separator (SiO_2 content = 5%). d) A comparison of liquid electrolyte wettability between PP/PE/PP separator and CNF separator. e) Thermal shrinkage (area-based dimensional change) of PP/PE/PP separator and CNF separator after exposure to 150 °C for 0.5 h. f–e) Reproduced with permission.^[88] Copyright 2013, Elsevier. f) A schematic illustration of functionalized CNF-integrated nanomat separator (c-mat) that consists of TPY-CNF thin layer and electrospun PVP/PAN support layer. g) High-temperature (60 °C) cycling performance of LiMnO_2 cathode-containing cells assembled with c-mat separator. f,g) Reproduced with permission.^[90] Copyright 2016, American Chemical Society.

electrolyte wettability (Figure 6d) and low thermal shrinkage at 150 °C for 0.5 h (Figure 6e). Stimulated by the functionalization of nanocellulose by its rich hydroxyl groups, a modified CNF-based battery separator was proposed.^[90] This separator was composed of a thin, nanoporous terpyridine (TPY)-functionalized CNF mat as a top layer and a thick, microporous polyvinylpyrrolidone (PVP)/polyacrylonitrile (PAN) mat as a support layer (Figure 6f). The TPY molecules were conjugated with the oxidized CNF to chelate unwanted byproducts (dissolved heavy metal ions from the cathode) in the electrolyte. The TPY-CNF separator with well-designed chemical functionality enabled a significant improvement in the high-temperature (e.g., 60 °C) cycling performance of LiMnO_2 -cathode-containing cells (Figure 6g).

6. Nanocellulose for Post-LIBs

In comparison to the supercapacitors and LIBs described above, the application of nanocellulose to newly emerging energy storage systems (so-called post-LIBs) such as lithium–sulfur (Li–S), sodium (Na)-ion, multivalent (magnesium, calcium, aluminum, and so on)-ion and metal–air batteries has rarely been reported. This indicates that nanocellulose may hold a promise as a competent building element that could address the stringent challenges of post-LIBs that remain unresolved with conventional battery materials and chemistries. Some representative examples of nanocellulose-based post-LIBs are briefly described below and are summarized in Table S4 (Supporting Information).

6.1. Nanocellulose for Li–S Batteries

Li–S batteries have received considerable attention due to their high theoretical energy density, low cost, and natural abundance of environmentally benign sulfur active materials.^[91–93] However, their practical application remains hinged on several challenges, such as the inherently poor electronic conductivity of sulfur and polysulfide-triggered shuttle phenomena that result in capacity decay, self-discharge, and low coulombic efficiency. Numerous efforts have been undertaken to address these issues, with a focus on sulfur electrodes, electrolytes, conductive interlayers, and separators. Nanocellulose can be used as a separator and an electrode binder or can be converted to carbon materials for Li–S batteries.^[94–97] Yu and co-workers^[94] reported sandwich-structured sulfur electrodes, which were welded in a CNT/CNF framework. The interconnected CNT/CNF layers effectively trapped polysulfide species and allowed facile electron transport (Figure 7a). N-doped graphene (NG) was used for sulfur electrodes, since hetero N-doping endows graphene with an improved electronic conductivity and polysulfide interception capability via coordination interactions. The resultant electrode exhibited good mechanical flexibility and robustness (inset image of Figure 7b). The CNT/CNF was entangled and interwoven, forming a 3D hierarchical network configuration (Figure 7b). The synergistic effects of physical encapsulation by the CNT/CNF and the chemisorption of polysulfides by NG resulted in good electrochemical performance (Figure 7c). The electrode with areal sulfur loading of 8.1 mg cm⁻² showed an areal capacity of ≈8 mA h cm⁻² and a capacity fading of 0.067% per cycle over 1000 cycles at a current rate of 0.5 C, while the average coulombic efficiency is around 97.3%. More recently, Lee and co-workers^[96] developed nanomat Li–S batteries based on all-fibrous cathode/separator assemblies and reinforced Li metal anodes to provide ultrahigh energy density and mechanical flexibility (Figure 7d). The bilayered paper separator (consisting of a CNF support layer and a negatively charged CNF active layer) was monolithically integrated with the sulfur cathode (fibrous mixtures of sulfur-deposited MWCNTs and SWCNTs), resulting in metallic foil current collector-free, all-fibrous cathode–separator assemblies. Driven by the anionic CNF (mitigating shuttle effect via electrostatic repulsion) and all-fibrous structure (providing bi-continuous ion/electron pathways), the nanomat Li–S batteries improved the redox kinetics, cyclability, and mechanical flexibility.

The porous carbon materials derived from nanocellulose can act as a conductive framework for Li–S batteries. Nazar and co-workers^[97] proposed dual-atom doped carbon with hierarchical porous structures derived from CNC (Figure 7e). The N,S-doped carbon with large surface area and high pore volume were fabricated by the liquid-crystal-driven self-assembly of polyrhodamine-coated CNC and the subsequent pyrolysis/etching of silica (silica precursors were added to provide space between particles and to avoid structural collapse upon carbonization). The dual-doping of porous carbon with N and S atoms greatly enhanced the chemisorption of polysulfides.

6.2. Nanocellulose for Na-Ion Batteries

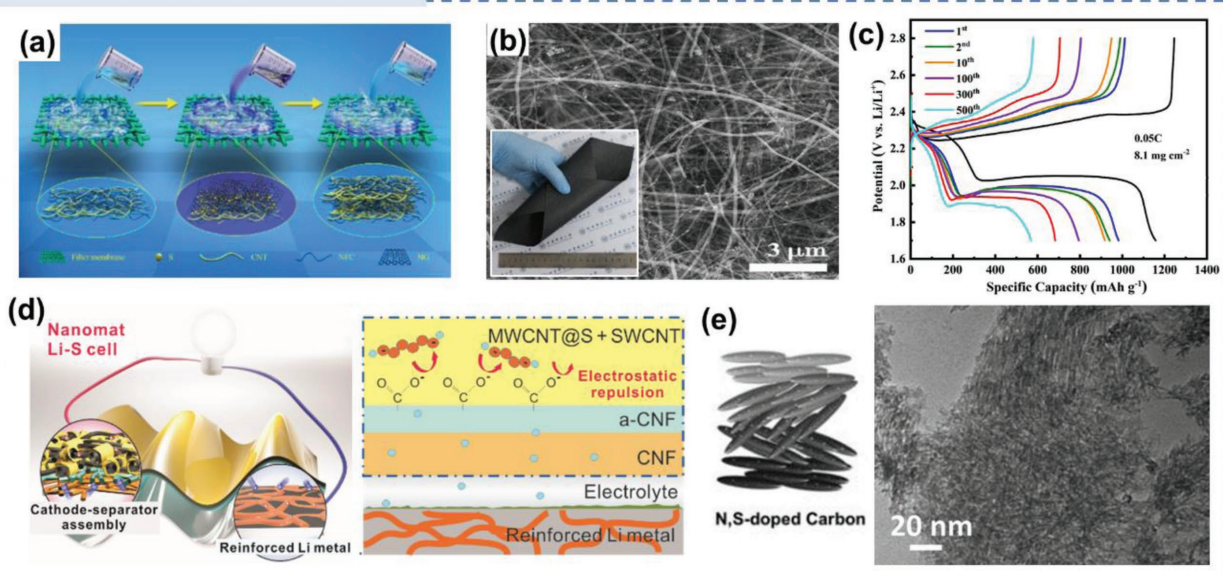
Na-ion batteries (SIB), owing to the natural abundance of Na, have been suggested as a promising system for low-cost

grid-scale ESSs. Tin (Sn) is known as a high-capacity SIB anode material and has a theoretical capacity of 847 mAh g⁻¹, however, it has several drawbacks such as large volume expansion during cycling, slow kinetics, and a poor formation of solid electrolyte interphase (SEI).^[98] Hu and co-workers^[99] reported a low-cost electrode composed of a Sn film electrodeposited on top of conductive wood fibers (Figure 7f). The coating of CNTs on the fiber surface enabled the electrical conductivity. The conductive wood fibers contributed to improving the cycling performance of the Sn anode, which can be explained by the suppression of electrode pulverization and by the facilitated ion diffusion kinetics. The soft nature of wood fibers released the mechanical stresses created by the sodiation, and the mesoporous structure served as an electrolyte reservoir, which thus allowed ion conduction through the inner and outer surfaces of the wood fibers. Nanocellulose-derived, heteroatom-doped carbon materials have shown advantages such as chemical and thermal stability, and electrical conductivity, as well as a high Na-ion storage capacity.^[100–104] As representative examples, N-doped,^[101] N, S-doped,^[102] N,O-doped,^[103] and B,N-doped porous carbon^[104] have been prepared from nanosized cellulose and successfully applied to SIB anodes (Figure 7g,h). Notably, the B,N-doped porous carbon^[104] enlarged the carbon layer spacing for Na⁺ insertion and improved the electrochemical activity, thereby providing a high specific charge capacity of 581 mAh g⁻¹ at 100 mA g⁻¹ after 120 cycles and a remarkable cycling stability with 277 mAh g⁻¹ at 10 A g⁻¹ after 1000 cycles.

6.3. Nanocellulose for Metal–Air Batteries

Metal–air rechargeable batteries are considered as one of the most competent next-generation power sources because of their half-opened configuration that consumes inexhaustible oxygen at air electrodes, leading to a high theoretical energy density.^[105,106] In metal–air rechargeable batteries, active and durable electrocatalysts that can accelerate the oxygen reduction reaction and evolution reaction (ORR and OER, respectively) play a decisive role in achieving electrochemical reliability. The electrocatalytic reaction rate is relatively slow and hence precious metals (e.g., Pt, Ru, and Ir) and their alloys have been exploited to overcome the sluggish kinetics and accelerate the electrochemical conversion process.^[107,108] However, the prohibitive cost and scarcity of precious metal-based electrocatalysts pose a formidable barrier to practical applications. To address these limitations, nanocellulose-derived air catalysts were recently suggested as cost-effective and precious-metal-free alternative electrocatalysts.^[107,109–112] Carbon materials produced from the pyrolysis of nanocellulose-derived materials possess electrochemically catalytic sites. Yu and co-workers^[109] reported a BC-derived nitrogen-doped carbon nanofiber aerogel ORR electrocatalyst for potential use in zinc (Zn)–air batteries, and it was prepared by the direct pyrolysis of freeze-dried BC, followed by NH₃ activation (Figure 7i). The resultant doped-N defects at the graphene edges and in-plane locations may act as active sites for the electrocatalysis of the ORR. Such a reasonable combination of fast transport path and high reactive surface area resulted in a superior ORR activity, high selectivity, and good electrochemical stability in alkaline media.

Nanocellulose for Li-S batteries



Nanocellulose for Na-ion batteries



Nanocellulose for metal-air batteries

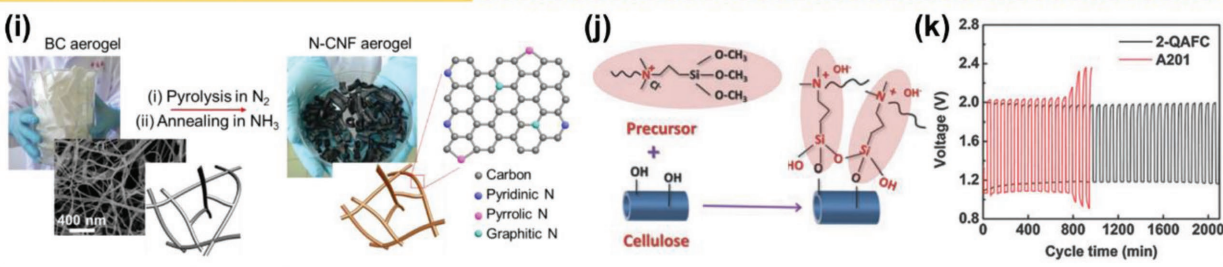


Figure 7. Nanocellulose for post-LIBs. a) A schematic of sandwich-structured sulfur cathodes containing CNT/CNF framework. b) SEM image of a NG-based sulfur cathode containing CNT/CNF framework. The inset shows its mechanical flexibility. c) Galvanostatic charge/discharge profiles of a NG-based sulfur cathode containing CNT/CNF framework. Reproduced with permission.^[94] Copyright 2017, Wiley-VCH. d) Conceptual illustrations of nanomat Li-S battery architecture and its contribution to electrochemical performance. Reproduced with permission.^[96] Copyright 2018, the Royal Society of Chemistry. e) An illustration and TEM image of CNC-derived N,S-doped carbons. Reproduced with permission.^[97] Copyright 2015, Wiley-VCH. f) A schematic of Sn-deposited conductive wood cellulose fiber electrode. Reproduced with permission.^[99] Copyright 2013, American Chemical Society. g) A schematic of N/S codoped carbon microspheres for SIB anodes. Reproduced with permission.^[102] Copyright 2016, Wiley-VCH. h) A schematic of fabrication process of BN-CNFs electrode from BC. Reproduced with permission.^[104] Copyright 2017, Wiley-VCH. i) A schematic of synthetic procedure of N-CNF aerogel for use in ORR electrocatalysts. Reproduced with permission.^[109] Copyright 2015, Elsevier. j) A schematic of surface-functionalized CNF with quaternary ammonium (CNF-based hydroxide-ion conductive electrolyte separator, named as 2-QAFC). k) Galvanostatic charge/discharge cycling behavior of 2-QAFC and A201 (control) membranes. j,k) Reproduced with permission.^[113] Copyright 2016, the Royal Society of Chemistry.

Chen and co-workers^[113,114] reported CNF-based alkaline anion-exchange membranes. The highly flexible and hydroxide-ion conductive electrolyte separator (named as 2-QAFC) was

fabricated through a surface-functionalization of CNF with quaternary ammonium (Figure 7j). The higher conduction of hydroxide ions and water retention of the membrane, and

also the low anisotropic swelling contributed to improving the specific capacities and cycling performance of the battery under atmospheric air, as compared to the commercial anion-exchange membrane (named as A201) (Figure 7k).

7. Summary and Future Outlook

In summary, we overviewed the recent research activities on nanocellulose as a green material opportunity for various energy storage systems. The structural uniqueness (characterized by the nanoscale dimension, 1D directionality, high specific surface area, and high crystallinity) and chemical functionalities of nanocellulose enabled exceptional performance improvements in the electrodes, electrolytes, separators, and architecture of the energy storage systems. Nanocellulose has been explored as a functional electrode element for supercapacitors. Various conducting materials such as CNTs, graphene, ECPs, and metal nanowires were combined with nanocellulose, resulting in the fabrication of electrochemically active paper/aerogel electrodes with structural uniqueness and mechanical flexibility. The nanocellulose-mediated porous morphology of paper/aerogel electrodes allowed for the construction of bicontinuous ion/electron transport pathways, thereby improving the electrochemical performance of the resultant supercapacitors. In addition, nanocellulose was used as a precursor for carbonaceous materials. In particular, the addition of heteroatom-containing substances during the carbonization of nanocellulose led to the preparation of heteroatom-doped carbonaceous materials with superior electrochemical properties, thus, contributing to higher specific capacitance than that of conventional carbons. Nanocellulose has been explored as an alternative electrode binder to outperform synthetic polymer binders for LIBs. To endow electronic conductivity, nanocellulose was physically/chemically combined with nanocarbons, producing a 3D porous conductive network in the electrode. The nanocellulose/nanocarbon-based conductive network allowed for the fabrication of paper electrodes free of binders, conductive additives, and metallic current collectors. The as-generated paper electrodes were lightweight and flexible and provided superior electrochemical performance over that of commercial electrodes. Nanocellulose has also been used as an ingredient of solid-state electrolytes and separator membranes to improve their mechanical properties, thermal stability, and dimensional integrity. Nanocellulose-derived carbon materials were also worked well for the electrodes of LIBs. The application of nanocellulose to newly emerging battery systems such as Li–S, Na-ion, multi-valent (magnesium, calcium, aluminum, and so on)-ion and metal–air batteries remains in the infant stage, suggesting the promise of nanocellulose as material that could address stringent challenges facing the new battery systems. For example, nanocellulose has been incorporated as an electrode binder and converted to carbonaceous materials. Notably, the conductive substrates and frameworks based on nanocellulose/carbon composites and heteroatom-doped carbon materials showed superiority in terms of chemical/thermal stability, electrical conductivity, and electrocatalytic activity compared to those of the pristine carbons.

Upon application to energy storage systems, nanocellulose has suffered from several drawbacks as follows: 1) Nanocellulose is not electrically conductive and thus needs to be integrated with conductive materials or be converted to carbon materials for use in electrodes and current collectors. 2) Nanocellulose is hydrophilic and has difficulty in integrating with hydrophobic active components. 3) Nanocellulose is dispersed predominantly in water solvent. Thus, removal of water is required to fabricate particles, fibers, films/nanopapers, and aerogels, however, this drying process is time-consuming and also demands complicated steps. 4) Mechanical strength and flexibility of some nanocellulose-derived materials are not yet sufficiently high for practical applications. For example, the CNC-derived films are fragile due to the low aspect ratio of CNC. The nanocellulose-derived carbon aerogels need further improvements in compressive strength and resilience. 5) For BC, it tends to be formed as a gel-like network structure and is not fluidic. For this reason, integration of BC with other active components overburdens mixing techniques. Furthermore, BC is still expensive and poses a concern for its practical applications. To ensure the persistent progress of nanocellulose-based energy storage systems and facilitate their commercial use, the following issues need to be addressed in the near future: 1) cost-competitive and large-scale production of nanocellulose from sustainable biomass resources through environmentally friendly processing routes, 2) facile integration of nanocellulose with various electrochemically active materials, 3) surface engineering of nanocellulose to enrich chemical functionalities, 4) interfacial control of nanocellulose with ion-/electron-conducting components and electrode active materials, 5) structural tailoring of nanocellulose-based materials/substrates for specific energy storage systems, 6) customized design of the chemistry/structure of nanocellulose for newly emerging energy storage systems, 7) manufacturing process compatibility with currently existing energy storage system technologies, and 8) value proposition of nanocellulose-based energy storage systems from a commercial point of view.

As described above, nanocellulose is highly anticipated to bring unprecedented benefits in the structure and performance of energy storage materials and systems over a wide range of electrochemistries, which lie far beyond those achievable with conventional synthetic materials. We envision that the ever-growing interests and research activities in nanocellulose for energy storage systems will move us closer toward a new eco-friendly smart/ubiquitous energy era, which will find the widespread popularity of nanocellulose-based power sources in various fields including flexible/wearable electronics, lightweight aircrafts (or drones), structural batteries, and low-cost ESSs.

Supporting Information

Supporting Information is available from the Wiley Online Library or from the author.

Acknowledgements

J.-H.K. and D.L. contributed equally to this work. This work was supported by the Basic Science Research Program (2017M1A2A2087810,

2018R1A2A1A05019733) and Wearable Platform Materials Technology Center (2016R1A5A1009926) through the National Research Foundation of Korea (NRF) funded by the Ministry of Science, ICT and future Planning. This work was also supported by the Industry Technology Development Program (10080540) funded by the Ministry of Trade, Industry & Energy (MOTIE, Korea) and also supported by the National Institute of Forest Science (FP 0400-2016-01).

Conflict of Interest

The authors declare no conflict of interest.

Keywords

bacterial cellulose, cellulose nanocrystals, cellulose nanofibrils, energy storage systems, nanocellulose

Received: July 27, 2018

Revised: September 17, 2018

Published online: December 18, 2018

- [1] M. Dresselhaus, I. Thomas, *Nature* **2001**, *414*, 332.
- [2] M. Armand, J.-M. Tarascon, *Nature* **2008**, *451*, 652.
- [3] B. Dunn, H. Kamath, J.-M. Tarascon, *Science* **2011**, *334*, 928.
- [4] N. S. Choi, Z. Chen, S. A. Freunberger, X. Ji, Y. K. Sun, K. Amine, G. Yushin, L. F. Nazar, J. Cho, P. G. Bruce, *Angew. Chem., Int. Ed.* **2012**, *51*, 9994.
- [5] S. Chu, A. Majumdar, *Nature* **2012**, *488*, 294.
- [6] M. R. Palacin, *Chem. Soc. Rev.* **2009**, *38*, 2565.
- [7] J. Lu, Z. Chen, Z. Ma, F. Pan, L. A. Curtiss, K. Amine, *Nat. Nanotechnol.* **2016**, *11*, 1031.
- [8] Y. Sun, N. Liu, Y. Cui, *Nat. Energy* **2016**, *1*, 16071.
- [9] J. W. Choi, D. Aurbach, *Nat. Rev. Mater.* **2016**, *1*, 16013.
- [10] X. Wang, X. Lu, B. Liu, D. Chen, Y. Tong, G. Shen, *Adv. Mater.* **2014**, *26*, 4763.
- [11] K.-H. Choi, D. B. Ahn, S.-Y. Lee, *ACS Energy Lett.* **2018**, *3*, 220.
- [12] Y. Habibi, L. A. Lucia, O. J. Rojas, *Chem. Rev.* **2010**, *110*, 3479.
- [13] R. J. Moon, A. Martini, J. Nairn, J. Simonsen, J. Youngblood, *Chem. Soc. Rev.* **2011**, *40*, 3941.
- [14] L. Jabbour, R. Bongiovanni, D. Chaussy, C. Gerbaldi, D. Beneventi, *Cellulose* **2013**, *20*, 1523.
- [15] H. Wei, K. Rodriguez, S. Rennekar, P. J. Vikesland, *Environ. Sci.: Nano* **2014**, *1*, 302.
- [16] X. Du, Z. Zhang, W. Liu, Y. Deng, *Nano Energy* **2017**, *35*, 299.
- [17] W. Chen, H. Yu, S.-Y. Lee, T. Wei, J. Li, Z. Fan, *Chem. Soc. Rev.* **2018**, *47*, 2837.
- [18] E. Sjostrom, *Wood Chemistry: Fundamentals and Applications*, Elsevier, San Diego, CA, USA **1993**.
- [19] D. Klemm, F. Kramer, S. Moritz, T. Lindström, M. Ankerfors, D. Gray, A. Dorris, *Angew. Chem., Int. Ed.* **2011**, *50*, 5438.
- [20] M. A. S. Azizi Samir, F. Alloin, A. Dufresne, *Biomacromolecules* **2005**, *6*, 612.
- [21] *The Fundamentals of Papermaking Materials: Transactions of the 11th Fundamental Research Symposium* (Ed: C. F. Baker), Pira International, Cambridge, UK **1997**.
- [22] L. Donaldson, *Wood Sci. Technol.* **2007**, *41*, 443.
- [23] H. Zhu, W. Luo, P. N. Ciesielski, Z. Fang, J. Zhu, G. Henriksson, M. E. Himmel, L. Hu, *Chem. Rev.* **2016**, *116*, 9305.
- [24] F. Jiang, T. Li, Y. Li, Y. Zhang, A. Gong, J. Dai, E. Hitz, W. Luo, L. Hu, *Adv. Mater.* **2018**, *30*, 1703453.
- [25] E. J. Foster, R. J. Moon, U. P. Agarwal, M. J. Bortner, J. Bras, S. Camarero-Espinosa, K. J. Chan, M. J. Clift, E. D. Cranston, S. J. Eichhorn, *Chem. Soc. Rev.* **2018**, *47*, 2609.
- [26] Y. Habibi, *Chem. Soc. Rev.* **2014**, *43*, 1519.
- [27] H. El-Saied, A. H. Basta, R. H. Gobran, *Polym.-Plast. Technol. Eng.* **2004**, *43*, 797.
- [28] P. Gatenholm, D. Klemm, *MRS Bull.* **2010**, *35*, 208.
- [29] M. Iguchi, S. Yamanaka, A. Budhiono, *J. Mater. Sci.* **2000**, *35*, 261.
- [30] R. Jonas, L. F. Farah, *Polym. Degrad. Stab.* **1998**, *59*, 101.
- [31] M. Foresti, A. Vázquez, B. Boury, *Carbohydr. Polym.* **2017**, *157*, 447.
- [32] W. Hu, S. Chen, J. Yang, Z. Li, H. Wang, *Carbohydr. Polym.* **2014**, *101*, 1043.
- [33] Y. Z. Zhang, Y. Wang, T. Cheng, W. Y. Lai, H. Pang, W. Huang, *Chem. Soc. Rev.* **2015**, *44*, 5181.
- [34] K. Gao, Z. Shao, X. Wang, Y. Zhang, W. Wang, F. Wang, *RSC Adv.* **2013**, *3*, 15058.
- [35] K. Z. Gao, Z. Q. Shao, J. Li, X. Wang, X. Q. Peng, W. J. Wang, F. J. Wang, *J. Mater. Chem. A* **2013**, *1*, 63.
- [36] Q. Y. Niu, K. Z. Gao, Z. Q. Shao, *Nanoscale* **2014**, *6*, 4083.
- [37] Q. Zheng, Z. Cai, Z. Ma, S. Gong, *ACS Appl. Mater. Interfaces* **2015**, *7*, 3263.
- [38] X. D. Zhang, Z. Y. Lin, B. Chen, S. Sharma, C. P. Wong, W. Zhang, Y. L. Deng, *J. Mater. Chem. A* **2013**, *1*, 5835.
- [39] Y. Liu, J. Zhou, E. W. Zhu, J. Tang, X. H. Liu, W. H. Tang, *J. Mater. Chem. C* **2015**, *3*, 1011.
- [40] M. Hamed, E. Karabulut, A. Marais, A. Herland, G. Nyström, L. Wägberg, *Angew. Chem., Int. Ed.* **2013**, *52*, 12038.
- [41] G. Nyström, A. Marais, E. Karabulut, L. Wägberg, Y. Cui, M. M. Hamed, *Nat. Commun.* **2015**, *6*, 7259.
- [42] G. Nystrom, A. Razaq, M. Stromme, L. Nyholm, A. Mihranyan, *Nano Lett.* **2009**, *9*, 3635.
- [43] Z. H. Wang, D. O. Carlsson, P. Tammela, K. Hua, P. Zhang, L. Nyholm, M. Stromme, *ACS Nano* **2015**, *9*, 7563.
- [44] H. Wang, E. Zhu, J. Yang, P. Zhou, D. Sun, W. Tang, *J. Phys. Chem. C* **2012**, *116*, 13013.
- [45] S. H. Li, D. K. Huang, B. Y. Zhang, X. B. Xu, M. K. Wang, G. Yang, Y. Shen, *Adv. Energy Mater.* **2014**, *4*, 1301655.
- [46] S. Y. Liew, W. Thielemans, D. A. Walsh, *J. Phys. Chem. C* **2010**, *114*, 17926.
- [47] A. Razaq, L. Nyholm, M. Sjödin, M. Stromme, A. Mihranyan, *Adv. Energy Mater.* **2012**, *2*, 445.
- [48] R. Liu, L. Ma, G. Niu, X. Li, E. Li, Y. Bai, G. Yuan, *Adv. Funct. Mater.* **2017**, *27*, 1701635.
- [49] X. Yang, K. Y. Shi, I. Zhitomirsky, E. D. Cranston, *Adv. Mater.* **2015**, *27*, 6104.
- [50] Z. Gui, H. L. Zhu, E. Gillette, X. G. Han, G. W. Rubloff, L. B. Hu, S. B. Lee, *ACS Nano* **2013**, *7*, 6037.
- [51] Z. Wang, P. Tammela, M. Stromme, L. Nyholm, *Adv. Energy Mater.* **2017**, *7*, 1700130.
- [52] A. Mihranyan, L. Nyholm, A. E. G. Bennett, M. Stromme, *J. Phys. Chem. B* **2008**, *112*, 12249.
- [53] A. Razaq, A. Mihranyan, K. Welch, L. Nyholm, M. Stromme, *J. Phys. Chem. B* **2009**, *113*, 426.
- [54] W. S. Chen, Q. Li, Y. C. Wang, X. Yi, J. Zeng, H. P. Yu, Y. X. Liu, J. Li, *ChemSusChem* **2014**, *7*, 154.
- [55] K. Y. Shi, X. Yang, E. D. Cranston, I. Zhitomirsky, *Adv. Funct. Mater.* **2016**, *26*, 6437.
- [56] K. H. Choi, J. Yoo, C. K. Lee, S. Y. Lee, *Energy Environ. Sci.* **2016**, *9*, 2812.
- [57] L. B. Hu, J. W. Choi, Y. Yang, S. Jeong, F. La Mantia, L. F. Cui, Y. Cui, *Proc. Natl. Acad. Sci. USA* **2009**, *106*, 21490.
- [58] L. B. Hu, M. Pasta, F. La Mantia, L. F. Cui, S. Jeong, H. D. Deshazer, J. W. Choi, S. M. Han, Y. Cui, *Nano Lett.* **2010**, *10*, 708.
- [59] V. Kuzmenko, O. Naboka, M. Haque, H. Staaf, G. Goransson, P. Gatenholm, P. Enoksson, *Energy* **2015**, *90*, 1490.

- [60] D. D. Shan, J. Yang, W. Liu, J. Yan, Z. J. Fan, *J. Mater. Chem. A* **2016**, *4*, 13589.
- [61] X. Xu, J. Zhou, D. H. Nagaraju, L. Jiang, V. R. Marinov, G. Lubineau, H. N. Alshareef, M. Oh, *Adv. Funct. Mater.* **2015**, *25*, 3193.
- [62] C. Chen, Y. Zhang, Y. Li, J. Dai, J. Song, Y. Yao, Y. Gong, I. Kierzewski, J. Xie, L. Hu, *Energy Environ. Sci.* **2017**, *10*, 538.
- [63] L. F. Chen, Z. H. Huang, H. W. Liang, H. L. Gao, S. H. Yu, *Adv. Funct. Mater.* **2014**, *24*, 5104.
- [64] L.-F. Chen, Z.-H. Huang, H.-W. Liang, W.-T. Yao, Z.-Y. Yu, S.-H. Yu, *Energy Environ. Sci.* **2013**, *6*, 3331.
- [65] X. Wu, Z. Shi, R. Tjandra, A. J. Cousins, S. Sy, A. Yu, R. M. Berry, K. C. Tam, *J. Mater. Chem. A* **2015**, *3*, 23768.
- [66] L. F. Chen, Z. H. Huang, H. W. Liang, Q. F. Guan, S. H. Yu, *Adv. Mater.* **2013**, *25*, 4746.
- [67] C. Long, D. Qi, T. Wei, J. Yan, L. Jiang, Z. Fan, *Adv. Funct. Mater.* **2014**, *24*, 3953.
- [68] Y. Jiang, J. Yan, X. Wu, D. Shan, Q. Zhou, L. Jiang, D. Yang, Z. Fan, *J. Power Sources* **2016**, *307*, 190.
- [69] L. Jabbour, C. Gerbaldi, D. Chaussy, E. Zeno, S. Bodoardo, D. Beneventi, *J. Mater. Chem.* **2010**, *20*, 7344.
- [70] L. Jabbour, M. Destro, D. Chaussy, C. Gerbaldi, N. Penazzi, S. Bodoardo, D. Beneventi, *Cellulose* **2013**, *20*, 571.
- [71] L. Hu, N. Liu, M. Eskilsson, G. Zheng, J. McDonough, L. Wågberg, Y. Cui, *Nano Energy* **2013**, *2*, 138.
- [72] S. Leijonmarck, A. Cornell, G. Lindbergh, L. Wågberg, *J. Mater. Chem. A* **2013**, *1*, 4671.
- [73] K.-H. Choi, S.-J. Cho, S.-J. Chun, J. T. Yoo, C. K. Lee, W. Kim, Q. Wu, S.-B. Park, D.-H. Choi, S.-Y. Lee, *Nano Lett.* **2014**, *14*, 5677.
- [74] S. J. Cho, K. H. Choi, J. T. Yoo, J. H. Kim, Y. H. Lee, S. J. Chun, S. B. Park, D. H. Choi, Q. Wu, S. Y. Lee, *Adv. Funct. Mater.* **2015**, *25*, 6029.
- [75] A. Du Pasquier, F. Disma, T. Bowmer, A. Gozdz, G. Amatucci, J. M. Tarascon, *J. Electrochem. Soc.* **1998**, *145*, 472.
- [76] Z. Chen, L. Christensen, J. Dahn, *J. Electrochem. Soc.* **2003**, *150*, A1073.
- [77] B. Wang, X. Li, B. Luo, J. Yang, X. Wang, Q. Song, S. Chen, L. Zhi, *Small* **2013**, *9*, 2399.
- [78] Y. Li, H. Zhu, F. Shen, J. Wan, X. Han, J. Dai, H. Dai, L. Hu, *Adv. Funct. Mater.* **2014**, *24*, 7366.
- [79] Y. Wan, Z. Yang, G. Xiong, H. Luo, *J. Mater. Chem. A* **2015**, *3*, 15386.
- [80] Y. Huang, Z. Lin, M. Zheng, T. Wang, J. Yang, F. Yuan, X. Lu, L. Liu, D. Sun, *J. Power Sources* **2016**, *307*, 649.
- [81] F. Zhang, Y. Tang, Y. Yang, X. Zhang, C.-S. Lee, *Electrochim. Acta* **2016**, *211*, 404.
- [82] C. Chen, Y. Zhang, Y. Li, Y. Kuang, J. Song, W. Luo, Y. Wang, Y. Yao, G. Pastel, J. Xie, L. Hu, *Adv. Energy Mater.* **2017**, *7*, 1700595.
- [83] Y. Zhang, W. Luo, C. Wang, Y. Li, C. Chen, J. Song, J. Dai, E. M. Hitz, S. Xu, C. Yang, Y. Wang, L. Hu, *Proc. Natl. Acad. Sci. USA* **2017**, *114*, 3584.
- [84] A. Chiappone, J. R. Nair, C. Gerbaldi, L. Jabbour, R. Bongiovanni, E. Zeno, D. Beneventi, N. Penazzi, *J. Power Sources* **2011**, *196*, 10280.
- [85] J. Zhang, C. Ma, Q. Xia, J. Liu, Z. Ding, M. Xu, L. Chen, W. Wei, *J. Membr. Sci.* **2016**, *497*, 259.
- [86] J. Chai, Z. Liu, J. Ma, J. Wang, X. Liu, H. Liu, J. Zhang, G. Cui, L. Chen, *Adv. Sci.* **2017**, *4*, 1600377.
- [87] S.-J. Chun, E.-S. Choi, E.-H. Lee, J. H. Kim, S.-Y. Lee, S.-Y. Lee, *J. Mater. Chem.* **2012**, *22*, 16618.
- [88] J.-H. Kim, J.-H. Kim, E.-S. Choi, H. K. Yu, J. H. Kim, Q. Wu, S.-J. Chun, S.-Y. Lee, S.-Y. Lee, *J. Power Sources* **2013**, *242*, 533.
- [89] J. Zhang, L. Yue, Q. Kong, Z. Liu, X. Zhou, C. Zhang, Q. Xu, B. Zhang, G. Ding, B. Qin, *Sci. Rep.* **2015**, *4*, 3935.
- [90] J.-H. Kim, M. Gu, D. H. Lee, J.-H. Kim, Y.-S. Oh, S. H. Min, B.-S. Kim, S.-Y. Lee, *Nano Lett.* **2016**, *16*, 5533.
- [91] A. Manthiram, Y. Fu, S.-H. Chung, C. Zu, Y.-S. Su, *Chem. Rev.* **2014**, *114*, 11751.
- [92] A. Manthiram, S. H. Chung, C. Zu, *Adv. Mater.* **2015**, *27*, 1980.
- [93] Q. Pang, X. Liang, C. Y. Kwok, L. F. Nazar, *Nat. Energy* **2016**, *1*, 16132.
- [94] M. Yu, J. Ma, M. Xie, H. Song, F. Tian, S. Xu, Y. Zhou, B. Li, D. Wu, H. Qiu, *Adv. Energy Mater.* **2017**, *7*, 1602347.
- [95] S. Li, T. Mou, G. Ren, J. Warzywoda, Z. Wei, B. Wang, Z. Fan, *J. Mater. Chem. A* **2017**, *5*, 1650.
- [96] J.-H. Kim, Y.-H. Lee, S.-J. Cho, J.-G. Gwon, H.-J. Cho, M. Jang, S.-Y. Lee, S.-Y. Lee, *Energy Environ. Sci.* **2018**, <https://doi.org/10.1039/c8ee01879k>.
- [97] Q. Pang, J. Tang, H. Huang, X. Liang, C. Hart, K. C. Tam, L. F. Nazar, *Adv. Mater.* **2015**, *27*, 6021.
- [98] S. W. Kim, D. H. Seo, X. Ma, G. Ceder, K. Kang, *Adv. Energy Mater.* **2012**, *2*, 710.
- [99] H. Zhu, Z. Jia, Y. Chen, N. Weadock, J. Wan, O. Vaaland, X. Han, T. Li, L. Hu, *Nano Lett.* **2013**, *13*, 3093.
- [100] W. Luo, J. Schardt, C. Bomnier, B. Wang, J. Razink, J. Simonsen, X. Ji, *J. Mater. Chem. A* **2013**, *1*, 10662.
- [101] Z. Zhang, J. Zhang, X. Zhao, F. Yang, *Carbon* **2015**, *95*, 552.
- [102] D. Xu, C. Chen, J. Xie, B. Zhang, L. Miao, J. Cai, Y. Huang, L. Zhang, *Adv. Energy Mater.* **2016**, *6*, 1501929.
- [103] M. Wang, Z. Yang, W. Li, L. Gu, Y. Yu, *Small* **2016**, *12*, 2559.
- [104] M. Wang, Y. Yang, Z. Yang, L. Gu, Q. Chen, Y. Yu, *Adv. Sci.* **2017**, *4*, 1600468.
- [105] P. Gu, M. Zheng, Q. Zhao, X. Xiao, H. Xue, H. Pang, *J. Mater. Chem. A* **2017**, *5*, 7651.
- [106] J. Fu, Z. P. Cano, M. G. Park, A. P. Yu, M. Fowler, Z. W. Chen, *Adv. Mater.* **2017**, *29*, 1604685.
- [107] F. Wang, T. Liu, Y. F. Guo, W. Z. Li, J. Qi, D. Rooney, K. N. Sun, *RSC Adv.* **2017**, *7*, 34763.
- [108] G. Wu, A. Santandreu, W. Kellogg, S. Gupta, O. Ogoke, H. G. Zhang, H. L. Wang, L. M. Dai, *Nano Energy* **2016**, *29*, 83.
- [109] H.-W. Liang, Z.-Y. Wu, L.-F. Chen, C. Li, S.-H. Yu, *Nano Energy* **2015**, *11*, 366.
- [110] S. Tong, M. Zheng, Y. Lu, Z. Lin, X. Zhang, P. He, H. Zhou, *Chem. Commun.* **2015**, *51*, 7302.
- [111] S. Liu, W. Yan, X. Cao, Z. Zhou, R. Yang, *Int. J. Hydrogen Energy* **2016**, *41*, 5351.
- [112] Y. Lu, G. Ye, X. She, S. Wang, D. Yang, Y. Yin, *ACS Sustainable Chem. Eng.* **2017**, *5*, 8729.
- [113] J. Fu, J. Zhang, X. P. Song, H. Zarrin, X. F. Tian, J. L. Qiao, L. Rasen, K. C. Li, Z. W. Chen, *Energy Environ. Sci.* **2016**, *9*, 663.
- [114] J. Zhang, J. Fu, X. P. Song, G. P. Jiang, H. Zarrin, P. Xu, K. C. Li, A. P. Yu, Z. W. Chen, *Adv. Energy Mater.* **2016**, *6*, 1600476.
- [115] B. Chen, N. Yang, Q. Jiang, W. Chen, Y. Yang, *Nano Energy* **2018**, *44*, 468.
- [116] S. Leijonmarck, A. Cornell, G. Lindbergh, L. Wågberg, *Nano Energy* **2013**, *2*, 794.
- [117] A. Malti, J. Edberg, H. Granberg, Z. U. Khan, J. W. Andreasen, X. Liu, D. Zhao, H. Zhang, Y. Yao, J. W. Brill, *Adv. Sci.* **2016**, *3*, 1500305.
- [118] Q. Jiang, C. Kacica, T. Soundappan, K.-k. Liu, S. Tadeppalli, P. Biswas, S. Singamaneni, *J. Mater. Chem. A* **2017**, *5*, 13976.
- [119] S. Y. Q. J. Y. Geng, P. J. Du Fengguo, *Sci. Silvae Sin.* **2012**, *2*, 029.
- [120] S. Ling, D. L. Kaplan, M. J. Buehler, *Nat. Rev. Mater.* **2018**, *3*, 18016.
- [121] K. Abe, H. Yano, *Cellulose* **2009**, *16*, 1017.